

Combining optimization and dynamic movement primitives for planning energy optimal forestry crane motions

Pedro La Hera¹, Daniel Ortiz Morales², Omar Mendoza-Trejo¹

¹Department of Forest Biomaterial and Technology, Section of Robotics and Automation, Swedish University of Agricultural Sciences, Umeå Campus, Umeå, Sweden

²CRANAB AB, Swedish Forestry Crane Manufacturing Company, Vindeln, Sweden

Article Info

Article history:

Received Nov 29, 2022

Revised Feb 20, 2024

Accepted Apr 8, 2024

Keywords:

Dynamic movement primitives

Energy optimization

Forestry crane automation

Motion optimization

Motion/trajectory planning

ABSTRACT

Forestry cranes are an important tool for safe and efficient timber harvesting with forestry machines. However, their complex manual control often led to inefficiencies and excessive energy usage, due to the many joysticks and buttons that must be used in a precise sequence to perform efficient movements. To address this, the industry is increasingly turning to partial automation, making manual control more intuitive for the operator and, consequently, achieving improvements in energy efficiency. This article introduces a novel approach to energy-optimal motion planning that can be used along with a feedback control system to automate crane motions, taking over portions of the operator's work. Our method combines dynamic movement primitives (DMPs) and an energy-optimization algorithm. DMPs is a machine learning technique for motion planning based on human demonstrations, while the optimization algorithm exploits the crane's redundancy to find energy-optimal trajectories. Simulation results show that DMPs can replicate human-like controlled motions with a 25% reduction in energy consumption. However, our energy optimization algorithm shows improvements of over 40%, providing substantial energy savings and a promising pathway towards environmentally friendly partially automated machines.

This is an open access article under the [CC BY-SA](https://creativecommons.org/licenses/by-sa/4.0/) license.



Corresponding Author:

Pedro La Hera

Department of Forest Biomaterials and Technology, Section of Robotics and Automation, Swedish

University of Agricultural Sciences, Umeå Campus, Umeå, Sweden

Email: xavier.lahera@slu.se

1. INTRODUCTION

In recent years, the forestry industry has seen a rise in the use of automation technologies to increase productivity and reduce human workload. One area that has received particular attention is the automation of forestry cranes, which are used for maneuvering heavy loads inside the forest. In a previous article, we introduced a motion planning method based on dynamic movement primitives (DMPs), in order to plan trajectories that can help operators execute portions of their crane work autonomously. In this article, we propose an additional optimization algorithm that can be used in conjunction with the DMP-based method to plan energy-optimal motions. By combining these two approaches, we aim to further improve the performance of partially automated forestry cranes in terms of energy efficiency and overall productivity.

Cut-to-length (CTL) timber harvesting is a modern logging method that involves felling trees and processing them into logs of specific lengths directly in the forest. This method uses specialized forestry machines equipped with advanced heavy-duty cranes, to harvest and process trees quickly and efficiently. Among these machines, two primary ones are known as the harvester and forwarder. The harvester uses a

harvesting head to cut the tree at the base and then cuts it into a log of a desired length, while the forwarder collects and transports logs from the harvesting site to the roadside landing. CTL timber harvesting is the primary method used in Fennoscandinavia, making this region one of the largest exporters of pulp and sawn timber [1].

While the use of heavy machines in forestry offers many benefits, efficient and safe control is critical to the success of the entire operation. These machines often have many joysticks, pedals, and buttons that must be used in the correct sequence to perform a specific task. Therefore, operating these machines can be challenging, as this requires a high degree of hand-eye coordination, spatial awareness, and mental focus for long periods of time. As this can be hard to master, the work with these machines leads to high energy consumption, environmental pollution [2], and long learning curves for new operators [3]–[5].

Research studies have shown that automation technology has the potential to improve the productivity and energy efficiency of forestry cranes [6]–[9]. This has led to an increased interest in automation technology among machine manufacturers, with examples including John Deere's Intelligent Boom Control, Komatsu Forest's Smart Flow and Smart Crane, and the intelligent hydraulic valves paving the way for the development of these new products [10]–[12]. These technologies are early versions of operator support technology that utilize automation software to facilitate manual control of forestry cranes. However, they do not exploit the full potential of automation, as they still require the operator to control every aspect of the crane work. Nonetheless, there are other advanced automation functions currently under research, such as the ability to perform autonomous motions as a complement to manual control [13], [14], which are attractive for today's market.

In [15], we introduced a framework for analyzing the patterns of how operators control crane motions while performing standard forwarding tasks. These tasks include picking up logs from the ground to the forwarder's trailer and unloading the logs at the landing area. Our study revealed that experienced operators have the ability to control cranes using repetitive motion patterns, resembling an automated system. This finding serves as our foundation for developing automated functions that simplify the operators' work, by letting a control system perform portions of the crane's motions autonomously. Building on this result, in [14], we present the first study of automating forwarder crane motions using machine learning. We proposed a motion-planning framework based on dynamic movement primitives (DMPs), a machine learning approach that teaches a system to mimic human motions [16] and can be used to generate smooth, adaptable, and robust movements. This is a technique that we believe is better suited to forestry than other standard motion-planning techniques used in robotics.

Many robotics applications, as summarized in [17], report that dynamic movement primitives (DMPs) are a useful tool in motion planning for several reasons. First, they provide a flexible and efficient way to learn and generalize movements from demonstrations. This means that a robot or machine can learn how to perform a task by observing a human or another machine perform the task, rather than relying on pre-programmed rules. Second, DMPs allow for easy modification of movement behavior in terms of speed and amplitude, which is crucial in dynamic environments where the robot or machine needs to respond quickly to changes in the environment. Third, DMPs are capable of adapting to external disturbances, which makes them more robust and adaptable in complex real-world environments. Finally, DMPs have a mathematical basis that allows for easy integration with other motion planning and control methods [16].

Our previous study [14] shows how DMPs can reliably reproduce human-like crane-controlled motions, but their performance is highly dependent on the quality of the demonstration dataset. One limitation of machine learning approaches like DMPs is that they can adopt suboptimal behaviors that exist in human demonstrations. In the case of forestry cranes, human operators struggle with multitasking and coordinating the control of all joints simultaneously, leading to inefficiencies in motion performance [4], [5], [18]. Thus, we can conclude that the motion data of cranes recorded with professional operators are likely to present similar inefficiencies [3]. This bottleneck in performance can be addressed by exploiting the crane's redundancy to produce optimal motions based on a performance criterion like energy. However, this is not directly part of the DMPs framework and requires additional optimization algorithms to be incorporated.

This article aims to build upon our previous study presented in [14] in the following way. Firstly, we introduce a novel approach to motion planning capable of generating energy-optimal motions. By integrating mathematical optimization into the DMPs, we seek to exploit the crane's redundancy to find alternative joint trajectories that minimize energy costs [19]. Our goal is to mimic the Cartesian space motions performed by machine operators while simultaneously identifying new joint trajectories having better energy performance.

Secondly, we aim to demonstrate the potential for significant energy savings using our proposed optimization method. Our approach has the potential to be used not only for planning energy-efficient motions in automation but also as a tool for training new machine operators in energy-efficient practices. Currently, machine operator training relies heavily on the teacher's experience, without any formal analysis

or guidance. By developing analysis tools such as ours, we hope to take the first step towards providing new operators with instruction and analysis of energy-efficient practices.

The example case of the motion planner presented here is to perform an autonomous motion to bring the logs back into the machine's trailer, once the operator has manually operated the crane to grab the logs from the ground. As outlined in [14], this is a progressive development step to be provided to machine operators as an autonomous function that can be accessed with the click of a button to reduce the operator's workload.

2. METHOD

2.1. Materials

2.1.1. Machine used for the study

The machine used for recording data is a Komatsu Forwarder 830 [20] equipped with a crane from the company CRANAB (model CRF 5.1) having a maximum length of 9.3 m when the crane is fully extended [21]. This machine has been used in many of our previous studies, e.g. [4], [13], [15]. Referring to Figure 1, the crane was equipped with four high resolution quadrature encoders able to measure the joint rotations with a resolution of 0.072 degrees (0.0012 rad) for the angular joints and 0.0007 m (0.7 mm) for the telescope. A real-time data acquisition unit (DAQ) was installed to record the data. This DAQ operated at a frequency of 1 KHz, i.e., 1,000 recordings per second.

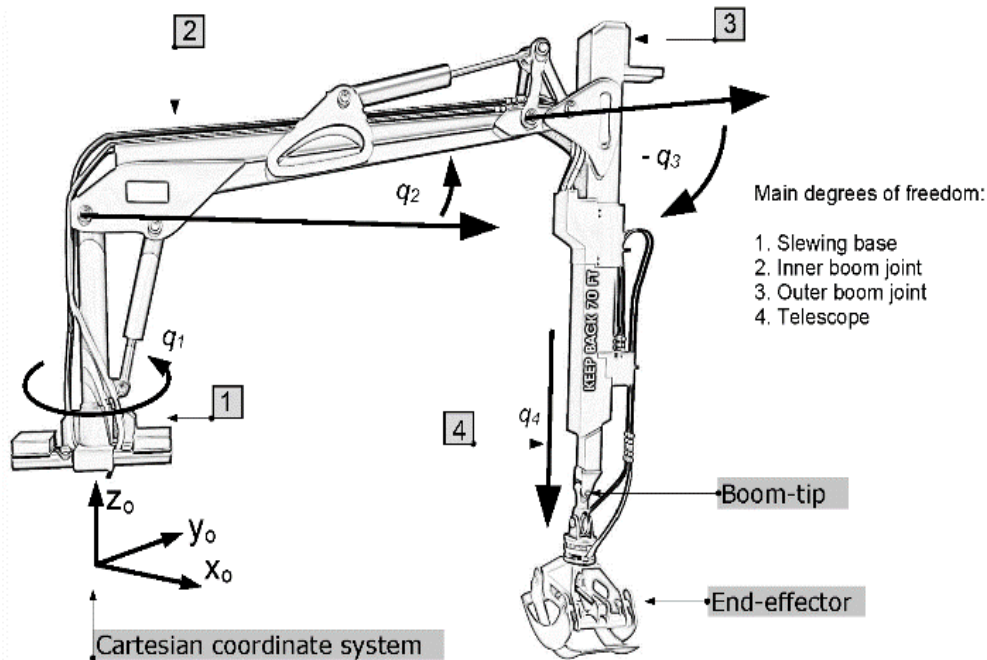


Figure 1. Forwarder crane [14]: hydraulic manipulator with four main degrees of freedom without counting the end-effector's tool; the sensors measure the joints known as the slewing q_1 , inner boom q_2 , outer boom q_3 , and telescope q_4 ; the end-effector tool is a grapple used to grab logs and it is attached to move freely at the boom-tip

2.1.2. Recorded data

As shown in Figure 2, the control of crane movements for loading logs involves two distinct actions that can be done on either side of the machine. The first action is to extend the crane from the trailer toward the logs for pick up. The second action is to return the crane loaded with logs back to the trailer. To avoid hitting the poles of the trailer, the return path is higher than the exit path, as can be observed in Figure 2. The exit path can be much lower because the crane can exit the trailer through the empty spaces between the poles to the sides. In the rest of the article, the exit and return paths are referred to as crane expanding and retracting motions.

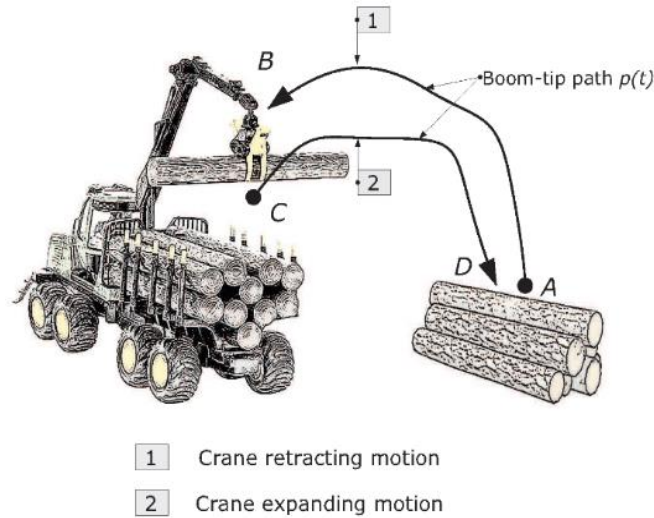


Figure 2. The paths described here refer to those for performing the actions of grabbing logs from one side of the machine, and accumulating them in the trailer [12]

2.1.3. Motion data set

Successful application of DMPs requires a rigorous data processing step that we perform off-line because when data is being recorded on a forestry machine, it does not have software that can automatically distinguish either the movements or the tasks being performed. Therefore, to make sense of recorded data, a crucial aspect of data processing is to separate the motions described in 2.1.2. This is done by trimming the data into individual tasks and arranging them in the form of vectors. This article is a continuation of our previous work on DMPs, and the data referenced here is the same as that presented in [15].

The data is shown in Figures 3 and 4. They correspond to the Cartesian trajectories of the boom tip and the telescopic link used to retract the crane from the left side of the vehicle. The dark bold signals are the averaged trajectories that are used in the learning process of the DMPs method. Figure 3 shows data plotted according to a monotonic parametric variable $\theta(t)$. This variable is the path curve length and it is shown in Figure 4 plotted with respect to time to show the duration of motions. Note that the duration of motion varies between trajectories because it depends on how much load the crane is holding: the higher the load, the slower the movement.

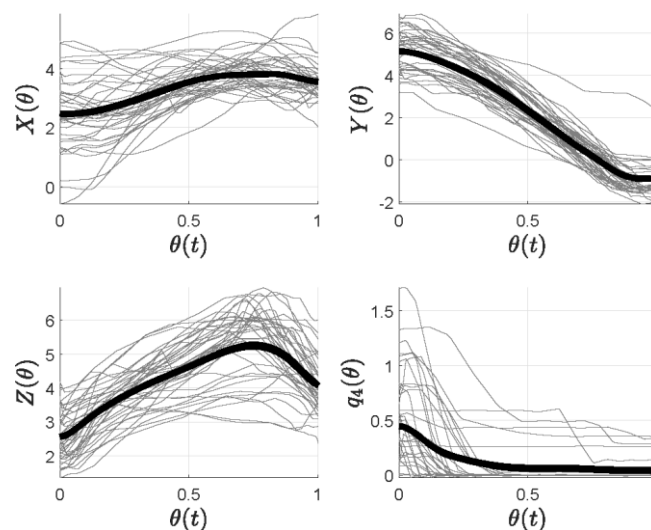


Figure 3. Cartesian coordinate trajectories $p(t)$ found after trimming the original data set, including the telescopic link q_4 . The bold signal represents the average of all trajectories [14]

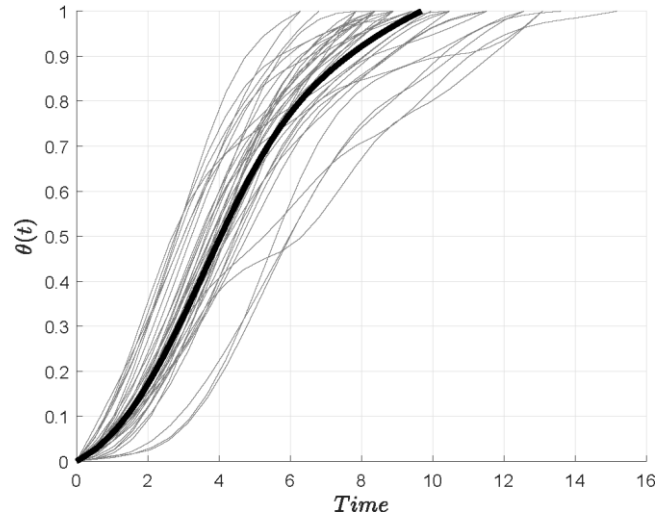


Figure 4. Normalized curve length in respect to time [14] (the bold signal is the averaged length used for interpolations)

2.2. Methods

We have chosen to work with dynamic movement primitives (DMPs) due to their various properties and successful applications reported in the field of robotics [16]. DMPs provide a formal mathematical framework for defining motion planners in terms of stable differential equations. Consequently, the solutions of these differential equations are used as desired trajectories and can be varied in velocities and amplitudes by simply changing the numerical values of some parameters [17]. In addition, this method satisfies some engineering requirements for industrial development. Specifically, DMPs are easy to implement in software, have low computational cost, and can be adapted by the machine operator without the need for coding. The following subsections provide the mathematical tools that are essential to apply DMPs.

2.2.1. Forward kinematics analysis

Referring to Figure 1, forwarder cranes are redundant manipulators composed of four main joints with one degree of redundancy [22]. The crane's open kinematic chain follows an RRRP convention, where the joints' positions measured through sensors can formally be written as the vector of generalized coordinates $q = [q_1, q_2, q_3, q_4]^T \in \mathfrak{R}$. Each of these joints is industrially referred to as: i) the slewing q_1 , ii) the inner boom q_2 , iii) the outer boom q_3 , and iv) the telescope q_4 .

The Cartesian coordinates of the boom tip as shown in Figure 2 can be calculated using the forward kinematics equation derived from the Denavit-Hartenberg (DH) convention [22]. Therefore, given the measurements of the generalized coordinates q , the boom-tip coordinates p can be explicitly given by (1)

$$p = \begin{bmatrix} x \\ y \\ z \end{bmatrix} = f(q) \quad (1)$$

where $f(q)$ is the forward kinematic equation detailed in [14].

2.2.2. Inverse kinematics analysis

Being a redundant manipulator, a closed-form solution to the inverse kinematics does not exist for this kind of crane [22]. However, given the fact that the crane resembles a two-link manipulator with variable length at the second link, a closed-form solution to the inverse kinematics problem can be given if the input data are the positions of the Cartesian boom-tip $p(q)$ and telescope q_4 . In such a case, the inverse kinematics can be formulated as (2),

$$q_{1,2,3} = F(p, q_4) \quad (2)$$

where the function $F(\cdot)$ to perform this calculation is detailed in [14]. Thus, having a specified path $p^*(t)$ and a trajectory for $q_4^*(t)$, the remaining degrees of freedom can be found explicitly through (2).

2.2.3. Mechanical power as a measurement of energy

Euler-Lagrange formulations help describe the crane dynamics as (3),

$$M(q)\ddot{q} + C(q, \dot{q})\dot{q} + G(q) = u \quad (3)$$

where $M(q)$ is a symmetric and positive-definite matrix of inertia, $G(q)$ is the gravity vector, and $C(q, \dot{q})$ is the matrix of Coriolis forces [22]. The right hand side u denotes the torques and forces required to perform a motion. Consequently, mechanical power can be computed from (4),

$$E = \int_0^T u(t) \cdot \dot{q}(t) dt \quad (4)$$

and it acts as a metric for the energy spent on motion, which correlates to fuel consumption [23]. Thus, torque can be calculated by replacing the values for joint positions $q(t)$, velocities $\dot{q}(t)$, and accelerations $\ddot{q}(t)$ in (3). Consequently, energy can be computed using (4) for the motion interval $t \in [0, T]$, having T as the time duration of the motion.

2.2.4. Dynamic movement primitive framework

As initially presented in [14], DMPs main concept is to use the following stable dynamical system for planning motions [16],

$$\begin{aligned} \tau \dot{n} &= \alpha_n (\beta_n (g - m) - n) + f \\ \tau \dot{m} &= n \end{aligned} \quad (5)$$

The desired trajectory's position, velocity, and acceleration are given by the values of $[m, \dot{m}, \ddot{m}]$ respectively. τ is a scaling constant that influences the velocity of the motion, and g is the goal position. f is a nonlinear forcing term determining the shape of the response. When $f=0$, the remaining system is a globally stable second-order linear system with $(n(T), m(T)) = (0, g)$ as unique point attractor from the initial state $=$, $m(0) = (n(0), m(0))$. The choice $\beta_n = \alpha_n/4$ makes (5) a critically stable damped system that converges monotonically towards the point attractor g [16].

The solution of the first-order canonical system,

$$\tau \dot{s} = -\alpha_s s, \quad (6)$$

defines the evolution of motion, removing the dependency on time. α_s is a constant that defines the monotonic rate of convergence from $s_0=1$ being the start of the motion, to $s_0 \approx 0$, being the proximity of the goal g . The complete system (5) and (6) has a unique equilibrium point at $(n, m, s) = (0, g, 0)$.

The purpose of DMPs is to find the nonlinear function f using human demonstrations, such that the solution of the system (5) and (6) resembles the demonstrated reference motion. To this end, the authors of [16] suggest a procedure using a machine learning approach based on Gaussian kernels. For our particular example, this approach is fully described in [14].

2.2.5. Training procedure applying the standard DMPs framework

For our purposes, using the DMPs framework for developing a motion planner consists of finding four differential equations of the form (5). These differential equations are for planning desired boom-tip path trajectories $[p^*t, \dot{p}^*t]$ and the desired telescope trajectory $[q_4^*(t), \dot{q}_4^*(t)]$. They can be formulated as (7) and (8).

$$\tau \ddot{p} = \alpha_n (\beta_n (q_p - p) - \dot{p}) + f_p \quad (7)$$

$$\tau \ddot{q}_4 = \alpha_n (\beta_n (q_{q_4} - q_4) - \dot{q}_4) + f_{q_4} \quad (8)$$

Consequently, the desired trajectories for the remaining degrees of freedom $[q_1^*(t), q_2^*(t), q_3^*(t)]$ can be found explicitly by calculating the inverse kinematics through (2). The data used for training the model (5) are shown by the bold black signals in Figure 3, corresponding to collecting logs from the left side of the vehicle. Nevertheless, forestry cranes perform similar motions to collect logs from either side of the machine. Therefore, it is sufficient to train the model with this data. Due to the properties of the model (5), all other variations of similar motions can be done consequently, irrespective of which side of the vehicle the motions are directed to, being an advantage of this approach. In the paragraphs below, we refer to the differential (7) and (8) found with the standard DMP framework as the standard motion planner.

2.2.6. Training procedure including energy optimization

Optimization of motion consists of exploiting the crane's redundancy to obtain optimal joint trajectories. One method consists in finding joint trajectories mimicking the paths $p(t)$ demonstrated by operators, but in a way that they minimize performance criteria involving energy in (4). To this end, our method is to find a better trajectory profile for the telescopic link $q_4(t)$ along the demonstrated path $p(t)$, because the trajectories for the remaining degrees of freedom can be found explicitly by calculating the inverse kinematics (2). This allows the operator to demonstrate suitable paths based on their experience, and better vision ability, while the optimization process finds the best energy-efficient joint trajectories to be used for the DMP approach.

As observed in Figures 2 and 3, the starting position of the telescope q_4 when grabbing a log depends on the habits of how the operator tends to manually control the crane. Typically, during the lifting motion, operators retract the telescope fully by the time the crane reaches the bunk [15]. As indicated in the work of [19], the initial condition of the telescope plays an important role in energy, because it affects the potential energy of the system. However, according to research studies [4], [15], machine operators are not able to use this link properly, because it demands multitasking and difficult coordination. As stated earlier, this inefficiency can be observed in data of the operator (see Figure 3), because the average telescope range of motion is within less than 20% of its maximum range. Thus, leaving plenty of space to exploit redundancy.

To optimize the motion, a method consists of finding a better initial condition $q_4(0)$ for (8) that can lead to minimizing energy. Thus, the only change with the optimization algorithm is the telescope's range of motion, as reusing (8) leads to motions having the same intrinsic properties taught by the machine operator. In addition, using a differential equation rather than a polynomial function reduces the complexity of the optimization search problem. To make sure that the telescopic link can close fast enough when starting from larger initial conditions (perhaps from a fully opened position), we can add a term to (8) in the form [16]:

$$f_a = k(m - 1.5 \cdot k) \left(\frac{1 \cdot \text{sign}(m - 1.5 \cdot k)}{2} \right) \quad (9)$$

resembling the behavior of an additional attractor, where f_a is the additional term, and k represents a spring-damper constant. The function involving sign is a mathematical form of an if-else command used to tell the system when to activate or deactivate this function. Thus, the new motion planner for q_4 has the form:

$$\tau \ddot{q}_4 = \alpha_n (\beta_n (g_{q_4} - q_4) - q) \quad (10)$$

In summary, the optimization task is to find the initial conditions $q_4(0)$ and the constant k for the optimization problem formulated as,

$$\min_{\{[q_4(0), k] \in \mathbb{R}\}} \frac{1}{2} E(q_4(0), k)^2$$

subject to

$$q_4^{\{min\}} < q_4(0) < q_4^{\{max\}} \quad (11)$$

$$k_{\{min\}} < k < k_{\{max\}} \quad (12)$$

$$u = M(q)\ddot{q} + C(q, \dot{q})\dot{q} + G(q) \quad (13)$$

$$\tau \ddot{q}_p = \alpha_n (\beta_n (g_p - p) - \dot{q}_p) + f_p \quad (14)$$

$$\tau \ddot{q}_{\{q_4\}} = \alpha_n (\beta_n (g_{\{q_4\}} - q_4) - \dot{q}_{\{q_4\}}) + f_{\{q_4\}} + f_a \quad (15)$$

$$q_{\{1,2,3\}} = F(p, q_4) \quad (16)$$

where $q_4^{\{min\}}$ and $q_4^{\{max\}}$ are the minimum and maximum ranges of the telescope. Similarly, $k_{\{min\}}$ and $k_{\{max\}}$ are minimum and maximum values for the constant k .

Notice that the differential equations working as motion planners for the Cartesian coordinates $p(t)$, given by (7), are still the same ones found with the standard training procedure described earlier. The

difference of an optimized motion planner is only the differential equation for $q_4(t)$, given by (10). In the paragraphs below, we refer to this new differential equation as the optimized motion planner.

2.2.7. Evaluation of motion planners

The following evaluations are designed to present a comparison between the performance between the standard and optimized motion planner against each other, and against data from the machine operator. To this end, this article presents two simulation cases.

Test 1 consists of simulating the standard and optimized motion planner using as initial conditions all those from the machine operator's demonstrated trajectories. A graphical representation of these initial conditions is sketched in Figure 5. The total energy is determined by summing up the energies of all trajectories. This process is performed a) for the standard motion planner, b) for the optimized motion planner, and c) for the machine operator. Consequently, a quantitative comparison of energy among these three cases can be provided. The objective is to assess the energy efficiency improvements achievable through automation as opposed to manual crane control by operators.

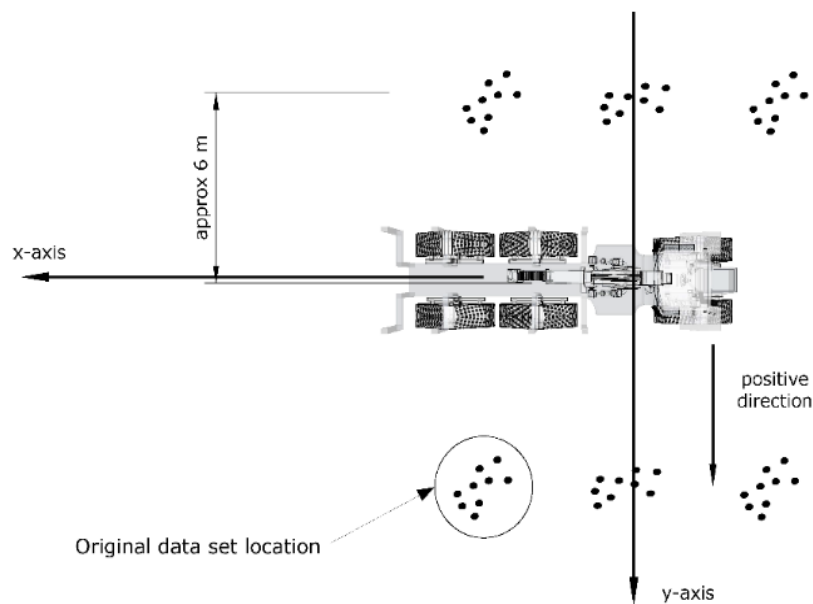


Figure 5. Different initial conditions for testing: dark dots represent the locations of the logs, from which the motion planning starts [15]

Test 2 consists of simulating the final motion planners using different initial conditions, resembling the act of collecting logs from different locations. These locations are chosen as the places where the machine operator grabs logs more frequently and would use the automatic motion planner to bring the logs into the machine's log bunk. Figure 5 depicts six different variations around the y-axis, located on both sides of the machine, selected based on the operator's crane control patterns [15]. It is assumed that five similar loads are collected at each location, giving a total of thirty motions. The goal is to demonstrate the motion planners' capability to handle differences in initial conditions, motion amplitude, and velocities, despite training with only one dataset. Additionally, the comparison of energy for the standard and optimized model's trajectories is presented to showcase their performance differences.

3. RESULTS AND DISCUSSION

3.1. Results of applying the DMPs framework

3.1.1. Final motion planning resulting from the standard DMPs framework

Figure 6 shows a comparison of the original data set and the desired trajectory as a result of using the standard motion planner given by (7) and (8). In the figure, the grey signals are the data set used for training the model, and the dashed black signals are the position trajectory using model (5). Results show the ability to replicate the averaged demonstration data set with a mean accuracy of 96.3%.

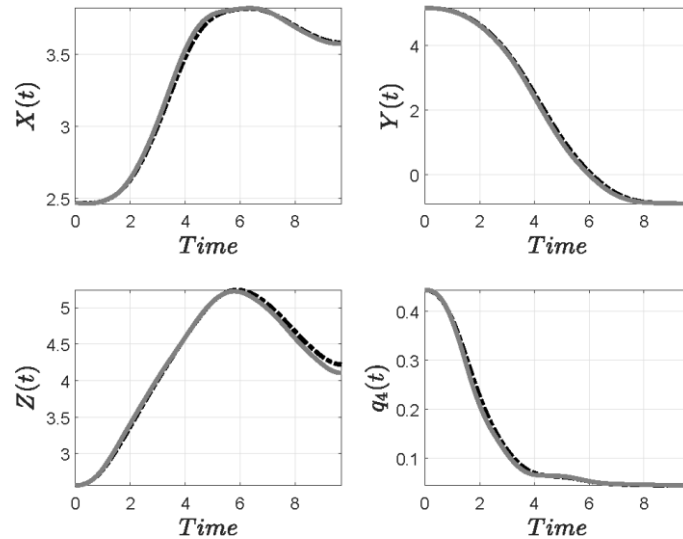


Figure 6. Comparison of the demonstrated position trajectories against the results of the motion planning model (5) [14]

3.1.2. Final motion planning after optimization

Referring to Figures 3 and 7, results show that the operator in this study uses the range of motion of the telescope within small ranges compared to its maximum. As explained in [15], this differs from operator to operator and it mainly depends on their multitasking skills. Nevertheless, using the telescope while coordinating the remaining joints is commonly difficult for machine operators.

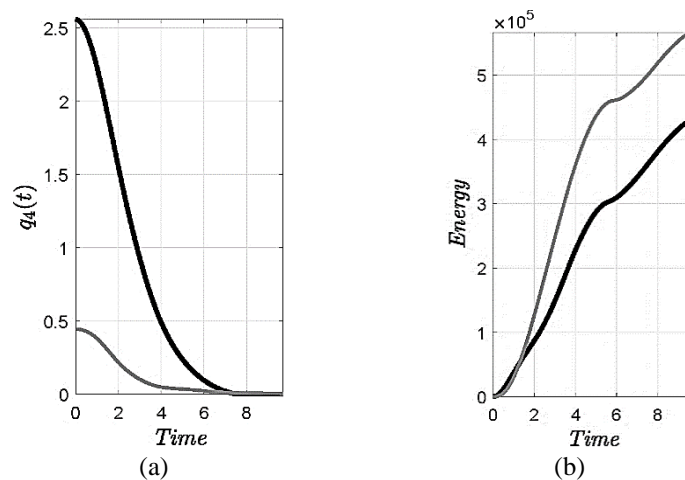


Figure 7. Results of (a) comparison of the standard and optimized telescope motion $q_4(t)$ and (b) calculation of energy as result of using these two variations (grey signal: standard motion planner, black signal: optimized one)

For the data used here, we see that the operator's averaged trajectory starts at nearly 12% of the maximum opening, i.e., $q_4(0)=0.4$ [m]. It is seldom that the operator uses up to nearly 50% of the opening of the telescope, i.e., $q_4(0)=1.7$ [m], as deduced from Figure 3. This leaves plenty of space where energy optimal motions may exist.

As described in section 2.2.6., we only modify the trajectory for the telescope $q_4(t)$ to optimize the motion over the operator's averaged path. For the optimization problem formulated by (16), the range for the telescope's initial conditions goes from $q^{min}=0$ to $q^{max}=3.5$ meters. The range for k is made half the telescope's maximum opening.

To solve this optimization problem, we use the optimization toolbox from MATLAB. Results of optimization are presented in Figure 7(a), showing that using the telescope around a range of 72%, i.e., $q_4(0)=2.5$ [m], provides energy saving in the range of 25%, as one can observe from Figure 7(b). The value found for $k=0.2$. Thus, results show that optimization has the ability to improve energy performance as we originally expected.

3.2. Simulation tests for evaluating the motion planners

3.2.1. Test 1: Total energy

Figure 8 shows an example comparing energy for a total of 38 trajectories out of the whole data set shown in Figure 3. The black bars represent the energy spent by the trajectories of the operator. The grey bars represent the energy spent by the trajectories from motion planning. Figure 8(a) is a graphical representation showing that the standard motion planner has the ability to reduce energy for most trajectories. However, it is notorious that the optimized motion planner, shown in Figure 8(b), can substantially reduce energy in relation to the standard case.

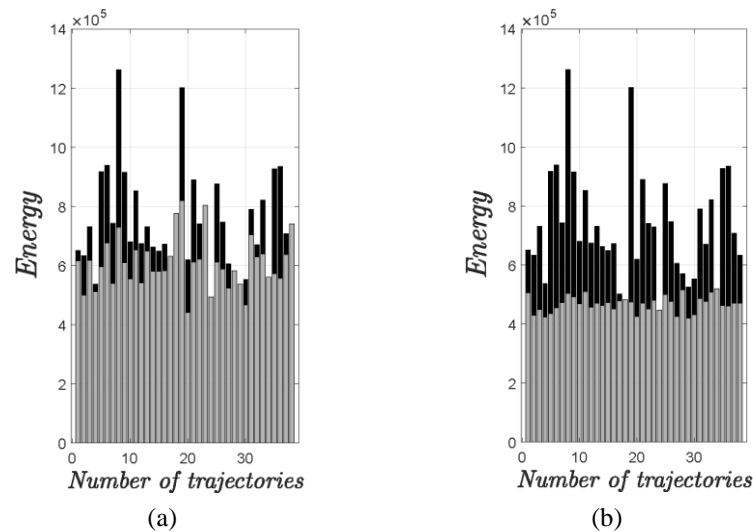


Figure 8. The comparisons of (a) the standard model energies in relation to the operator's trajectories and (b) the optimized model energies in relation to the operator's trajectories (grey: the DMPs model, black: operator's data)

Overall, the standard motion planner shows a 25% improvement in energy efficiency over trajectories produced by the operator when considering all of the trajectories in the data set displayed in Figure 3. In contrast, the optimized motion planner surpasses the machine operator by planning motions that consume 40% less energy. These results demonstrate that both the standard and optimized motion planners can reduce energy consumption, but the optimized planner achieves higher energy savings, averaging 15% better than the standard planner. Notably, as observed in Figure 8(b), most crane motions require a comparable amount of energy when using the optimized motion planner.

3.2.2. Test 2: Different initial conditions

This test shows the ability of both models to handle the uncertainty in initial conditions, i.e., the ability to plan motions from any desired position. The results are based on initial conditions visually sketched in Figure 5. The results of this simulation are presented in Figure 9, displaying the paths in Cartesian space.

The individual joint trajectories for the standard and optimized model are shown in Figure 10. The difference between the trajectories planned by these models is observed in the plot for the telescopic link q_4 , which contains different initial conditions according to the standard and optimized motion planners. To understand the benefits of the optimized motion planner, Figure 11 shows the energy comparison. The black bars represent the energy for the motions planned by the standard motion planner, while the grey bars are for the optimized case. In average, the optimized case behaves 12% better than the standard one, when considering the total energy of all trajectories.

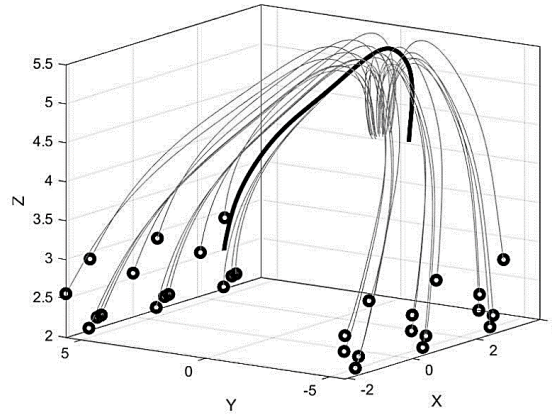


Figure 9. Cartesian coordinate plot for all simulated paths (grey signals: trajectories planned by the model (5), dark dots: new initial conditions used for the simulation, solid bold line: the path used as data set for learning)

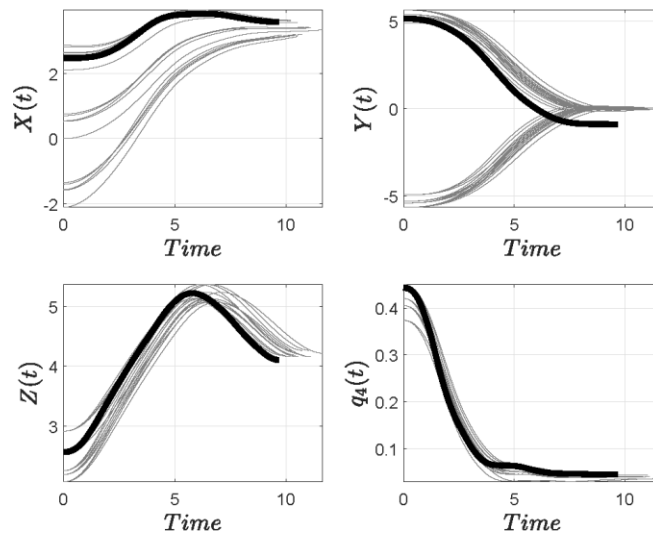


Figure 10. The grey signals are the trajectories planned by the model (5) (solid bold lines: trajectories used as data set for learning)

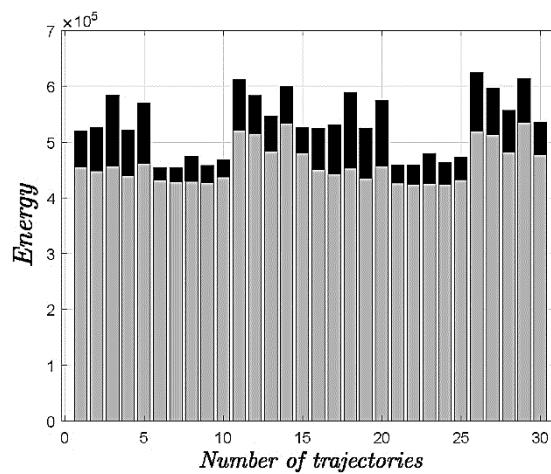


Figure 11. Comparison of the standard model energies in relation to the optimized model (grey signal: the energy of the optimized model, black signal: the energy of the standard model)

3.3. Discussion

Dynamic movement primitives are useful frameworks to develop dynamic motion planners based on demonstrated actions. In [14], we examined the standard application of DMPs for performing one particular action, i.e., bringing the crane loaded with logs into the machine automatically once an operator has grabbed them using joysticks. We argued that this action is a feasible incremental step in automation functions to be provided to machine operators in the near future.

In this article, our study was centered on proposing a complementary method to apply the DMP framework, with the purpose of developing a motion planner capable of planning energy-optimal motions. The argument for using optimization is that human demonstrations in this kind of machine can have some inherited inefficiencies due to the complex manual control involved in them. Therefore, our contribution is to incorporate an optimization routine used to exploit the crane's redundancy for developing a motion planner able to plan trajectories having better energy characteristics. In this way, the new motion planner is able to replicate human-like controlled motions in Cartesian space, but it is able to exploit redundancy in the joint space to achieve better energy performance. These results are novel within the context of applying DMPs and can be expanded to plan motions meeting different performance criteria specifications than the one used in this article.

3.3.1. Discussion about results

The first objective of the study was to determine to what extent the motion planner could replicate the demonstration data set. The results showed that the motion planner, using the standard DMP framework, was able to reproduce the demonstrated motion with over 95% accuracy. However, the operator's habit of using the telescopic link within only 12% of its maximum range may not lead to energy-optimal motions.

To improve energy efficiency, an optimization procedure was proposed and applied to the motion planner. The results showed that the optimized motion planner was able to save 40% energy while reproducing the same Cartesian motion as the demonstration data set. To this end, the optimized motion planner used the telescopic link within 72% of its maximum range. These findings demonstrated that using unusual joint movements in the motion planner could help optimize energy usage and that modifying the DMP framework could provide the motion planner with the ability to exploit redundancy to meet performance specifications.

To further explore the benefits of motion planners, two different tests were performed. The first test quantified the total energy consumption of all trajectories shown in Figure 3. The standard motion planner provided better energy performance than the operator's motions, reducing energy consumption by almost 25%. The optimized motion planner achieved even better performance, reducing energy consumption by nearly 40%. The second test involved simulating a scenario of collecting logs from different initial points, as shown in Figure 5. Both motion planners were able to adapt to different initial conditions and reproduce motions similar to the demonstration data set. However, the optimized motion planner had better energy performance than the standard one, achieving a 12% energy reduction.

Lower energy consumption in forestry machines translates to lower emissions and fuel consumption, which are important environmental factors for manufacturers. The study showed that automation can bring benefits to the forestry industry by improving both productivity and energy efficiency. Instructing operators to handle standard cranes based on analytical methods can lead to further increases in productivity and efficiency in manual operation. Training simulators can be programmed with tools that help students practice imitating energy-optimal joint reference trajectories, leading to better education for operators.

4. CONCLUSION

In conclusion, this study has demonstrated that combining the DMP framework with mathematical optimization can substantially improve energy efficiency in automated forestry crane motions. By exploiting redundancy in crane movements, the motion planner can reduce energy consumption by up to 40% compared to traditional operator-controlled motions. The potential benefits of these findings include the possibility of improving energy efficiency in partially automated forestry machines, as well as providing a potential tool for training new machine operators. However, the study also acknowledges several limitations that must be addressed, including the need for motion feedback control systems to execute the motions planned by the DMP algorithm and the current lack of computer vision systems in forestry machines. At present, our motion planner is blind, because computer vision systems are not available in forestry machines, and it will take a while for them to become available in this industry. Therefore, the application of our approach is directed towards the Scandinavian cut-to-length system, which leads to obstacle-free work for forwarder cranes. Additionally, the energy improvements reported are subjective and may vary across different operators.

Nevertheless, similar findings will exist when analyzing any machine operator, as the work with forestry cranes is today not necessarily efficient.

ACKNOWLEDGEMENTS

The authors would like to acknowledge the support of the company “The Swedish Cluster of Forest Technology” (in Swedish: Skogstekniska Klustret) for their help in getting the machine to record the data used in this article. Similarly, we would like to acknowledge the technical help of the company Komatsu Forest for placing the sensors in the forwarder machine used in the study. Acknowledgments to Prof. Ola Lindroos for his support in acquiring the financial support to carry on with this study. The authors gratefully acknowledge the financial support of the Kempe Foundation.

This study was partly financed by the Swedish Foundation for Strategic Environmental Research MISTRA (program MISTRA Digital Forest), the Kempe Foundations (project JCK-1713), and the Swedish Cluster of Forest Technology.

REFERENCES

- [1] E. Liski, P. Jounela, H. Korpunen, A. Sosa, O. Lindroos, and P. Jylhä, “Modeling the productivity of mechanized CTL harvesting with statistical machine learning methods,” *International Journal of Forest Engineering*, vol. 31, no. 3, pp. 253–262, Sep. 2020, doi: 10.1080/14942119.2020.1820750.
- [2] E. R. Labelle and K. J. Lemmer, “Selected environmental impacts of forest harvesting operations with varying degree of mechanization,” *Croatian Journal of Forest Engineering*, vol. 40, no. 2, pp. 239–257, Jul. 2019, doi: 10.5552/crojfe.2019.537.
- [3] M. B. Pagnussat, E. da Silva Lopes, and R. D. Seidler, “Behavioural profile effect of forestry machine operators in the learning process,” *Journal of Forest Science*, vol. 65, no. 4, pp. 144–149, Apr. 2019, doi: 10.17221/27/2019-JFS.
- [4] D. O. Morales, P. La Hera, S. Westerberg, L. B. Freidovich, and A. S. Shiriaev, “Path-constrained motion analysis: an algorithm to understand human performance on hydraulic manipulators,” *IEEE Transactions on Human-Machine Systems*, vol. 45, no. 2, pp. 187–199, Apr. 2015, doi: 10.1109/THMS.2014.2366873.
- [5] T. Nurminen, H. Korpunen, and J. Uusitalo, “Time consumption analysis of the mechanized cut-to-length harvesting system,” *Silva Fennica*, vol. 40, no. 2, pp. 335–363, 2006, doi: 10.14214/sf.346.
- [6] R. Visser and O. F. Obi, “Automation and robotics in forest harvesting operations: Identifying near-term opportunities,” *Croatian Journal of Forest Engineering*, vol. 42, no. 1, pp. 13–24, Aug. 2021, doi: 10.5552/crojfe.2021.739.
- [7] P. M. B. Torres, G. Spencer, L. Neto, G. Gonçalves, and R. Dionisio, “Industrial digitalization solutions for precision forestry towards forestry 4.0,” in *Lecture Notes in Networks and Systems*, vol. 629 LNNS, Springer International Publishing, 2023, pp. 79–86.
- [8] J. Reitz, M. Schluse, and J. Roßmann, “Industry 4.0 beyond the factory: an application to forestry,” in *Tagungsband des 4. Kongresses Montage Handhabung Industrieroboter*, Springer Berlin Heidelberg, 2019, pp. 107–116.
- [9] J. Manner, A. Mörk, and M. Englund, “Comparing forwarder boom-control systems based on an automatically recorded follow-up dataset,” *Silva Fennica*, vol. 53, no. 2, 2019, doi: 10.14214/sf.10161.
- [10] “Crane control systems,” *Techion Hydac International*. <https://technion.fi/> (accessed Jul. 01, 2022).
- [11] F. Reuter, “Komatsu SmartFlow – new hydraulic system for forwarder,” *NordicWoodJournal*, 2017. <https://nordicwoodjournal.com/editorial/equipments/komatsu-smartflow-hydraulic-system-forwarder/>.
- [12] “EATON, <https://www.eaton.com/gb/en-gb/catalog/valves/cma-advanced-mobile-valves.models.html>, Accessed in 2024.”
- [13] D. O. Morales, S. Westerberg, P. X. La Hera, U. Mettin, L. Freidovich, and A. S. Shiriaev, “Increasing the level of automation in the forestry logging process with crane trajectory planning and control,” *Journal of Field Robotics*, vol. 31, no. 3, pp. 343–363, Jan. 2014, doi: 10.1002/rob.21496.
- [14] P. La Hera, D. O. Morales, and O. Mendoza-Trejo, “A study case of dynamic Motion Primitives as a motion planning method to automate the work of forestry cranes,” *Computers and Electronics in Agriculture*, vol. 183, Apr. 2021, doi: 10.1016/j.compag.2021.106037.
- [15] P. La Hera and D. O. Morales, “What do we observe when we equip a forestry crane with motion sensors?,” *Croatian Journal of Forest Engineering*, vol. 40, no. 2, pp. 259–280, Jul. 2019, doi: 10.5552/crojfe.2019.501.
- [16] M. Saveriano, F. J. Abu-Dakka, A. Kramberger, and L. Peternel, “Dynamic movement primitives in robotics: a tutorial survey,” *International Journal of Robotics Research*, vol. 42, no. 13, pp. 1133–1184, Sep. 2023, doi: 10.1177/02783649231201196.
- [17] H. Ravichandar, A. S. Polydoros, S. Chernova, and A. Billard, “Recent advances in robot learning from demonstration,” *Annual Review of Control, Robotics, and Autonomous Systems*, vol. 3, no. 1, pp. 297–330, May 2020, doi: 10.1146/annurev-control-100819-063206.
- [18] H. Kymäläinen, T. Hujala, C. Häggström, and J. Malinen, “Workability and productivity among CTL machine operators—associations with sleep, fitness, and shift work,” *International Journal of Forest Engineering*, vol. 34, no. 3, pp. 426–438, May 2023, doi: 10.1080/14942119.2023.2216113.
- [19] T. Sandakalum and M. H. Ang, “Motion planning for mobile manipulators—a systematic review,” *Machines*, vol. 10, no. 2, Jan. 2022, doi: 10.3390/machines10020097.
- [20] “Komatsu Forest AB, ‘Forwarder 830.3,’ <http://www.komatsuforest.se>, Accessed in 2024.”
- [21] “Cranab, ‘Cranab presents an entirely new generation of cranes,’ <https://www.mynewsdesk.com/se/cranab-ab/pressreleases/cranab-presents-an-entirely-new-generation-of-cranes-647451>, Accessed in 2024.”
- [22] M. W. Spong, S. Hutchinson, and M. Vidyasagar, “Robot modeling and control,” *IEEE Control Systems*, vol. 26, no. 6, pp. 113–115, Dec. 2006, doi: 10.1109/MCS.2006.252815.
- [23] A. Tansini, G. Fontaras, B. Ciuffo, F. Millo, I. Prado Rujas, and N. Zacharof, “Calculating heavy-duty truck energy and fuel consumption using correlation formulas derived from VECTO simulations,” Apr. 2019, doi: 10.4271/2019-01-1278.

BIOGRAPHIES OF AUTHORS

Pedro La Hera     received his Ph.D. degree in Applied Physics and Electronics from the University of Umeå, Sweden, in 2011. He majored in control systems, and his main field of work is robotics and computational intelligence. Currently, he works as an associate professor in the section of Forest Technology at the Swedish University of Agricultural Sciences. His main research directions include intelligent motion control of heavy-duty hydraulic systems, artificial intelligence, computational intelligence, motion planning, and optimization. Over the past decade, he has been working with industry and academia to transform heavy-duty machines into smart systems. He can be contacted at xavier.lahera@slu.se.



Daniel Ortiz Morales     received the M.Sc. and Ph.D. degrees in robotics and control engineering from Umeå University, Sweden, in 2009 and 2015, respectively. Since then, he has been working as an automation engineer for industrial companies developing heavy-duty hydraulic manipulators. Currently, he works developing smart motion control systems for the Swedish crane manufacturing company CRANAB AB. He can be contacted at daniel.ortiz.morales@cranab.se.



Omar Mendoza-Trejo     received a B.S. degree in industrial robotics engineering from ESIME-IPN, Mexico City, Mexico, in 2010, and the M.Sc. and Ph.D. degrees in electrical engineering from CINVESTAV-IPN, Mexico City, Mexico, in 2012 and 2017, respectively. His research interests include the design of mechatronic systems using mathematical optimization and smart motion control systems. He is currently a researcher at the Forest Technology Department, Swedish University of Agricultural Sciences, Umeå, Sweden. He can be contacted at omar.mendoza.trejo@slu.se.